Adequacy of Finite Element Analysis in Numerical Simulation and Behaviour Prediction of RC Beam and Post Tensioned Slab in Fire Tests

Sajid Ahmad Mulani [a,*], Sachin Kadam [a], Athar Jamadar [b]

[a] Department of Applied Mechanics, Walchand College of Engineering, Sangli, Maharashtra, India
[b] Department of Civil Engineering, Kasegaon Education Society's Rajarambapu Institute of Technology, affiliated to Shivaji University, Sakharale, MS-415414, India

Corresponding author: [*]sajidahmad.mulani@walchandsangli.ac.in

Abstract—**Finite Element analysis has evolved into a crucial method for predicting behaviour of civil structures in real world. Because concrete depreciates quickly at high temperatures in terms of its mechanical, chemical, physical, and thermal properties, fire poses a serious hazard to reinforced concrete structures. The duration to which the structure is exposed to fire determines the maximum temperature it will attain. Experimental fire tests are not financially feasible and resource-intensive, and the size of specimen is to be tested is limited by the testing facility's capability. Furthermore, because the structure's many components are subjected to varying temperatures, the behaviour of the specimen is not a true representation of entire structure. Finite Element Analysis has been demonstrated to be beneficial in tackling this since it makes complex structural models and loading conditions easy to apply, thus facilitating the forecasting of their behaviour. This research study evaluates the efficiency of Finite Element analysis in predicting the behaviour of various structural components subjected to fire by comparing them with Experimental results.**

Keywords—**Elevated temperatures; numerical simulation; finite element analysis; mechanical properties; stress-strain curves.**

I. INTRODUCTION

As urban areas increasingly embrace high-rise construction with post-tensioned being the preferred choice, understanding the behaviour of these buildings in fire incidents becomes crucial. The US Fire Administration's 2022 [1] report identifies cooking as the primary cause of residential fires, highlighting significant losses and incident frequency in Figure 1.The losses due to fire cases have significantly increased over the last decade while the fire cases show a slight decline over the decade.

This study focuses on assessing how post-tensioned slabs and RC beam perform under fire conditions. It aims to provide insights into the structural integrity and safety of modern urban buildings. By doing so, the research aims to inform better safety measures and building codes, ensuring these structures can effectively manage and mitigate fire risks, thereby safeguarding residents and properties. Over the years many researchers have studied the effect of fire on built-up environments. Fire hazard in buildings can be defined as the potential of accidental or intentional fire to threaten life, structural, and property safety in a building [2]. Only recorded structural failures in tall buildings are due to earthquakes and fire, while a lot of research is done to ensure the proper safety of tall buildings against earthquakes very less studies exist against fire. In recent years the collapse of the World Trade Centre and the partial collapse of Windsor Tower in Spain are some examples of Structural Damage due to Fire. Cowlard A explained how fire travels through tall buildings vertically through compartmentation. The deformation of the system as a whole when exposed to fire can expose gaps and flammable materials which can lead to spread both upwards through flaming, and downwards through dripping molten materials [3].

Post-tensioned slabs unlike normal RC slabs have highly stressed reinforcement called strands which are subjected to large tensile stresses. These tensile stresses generated in tendons are used to carry the self-weight of slab. Thus, compared to normal RC Flat slab fewer bending moments and shear forces are generated in post-tensioned slab sections due to live loads. Also Prestressed slabs are subjected to high loads, and tendons used are highly stressed during their

lifetime. Any case of fire damage may lead to premature tendon failure and localized collapse of slabs [4]. Even minor or moderate damage to the main structural system with severe damage to the floor system can even lead to the loss of the building's usability after fire. [5]. Prestressing bars undergo high-strength deterioration when compared with reinforcement bars at elevated temperatures [6], [7] and this occurs due to the formation of pearlite from martensite [8].
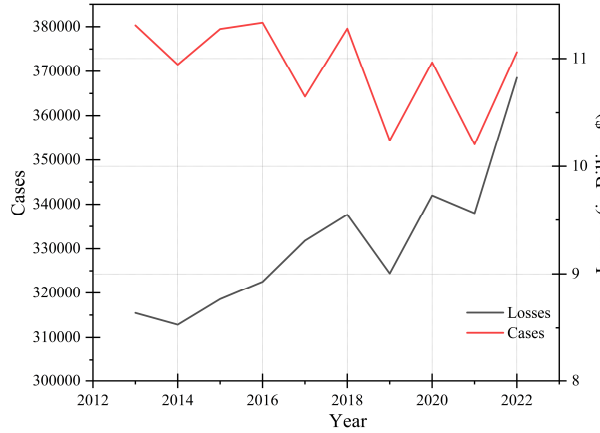

Fig. 1 Losses and Frequency of Fire Cases [1]

A. Fire Curves

Earthquake hazard acts as waves with positive and negative amplitudes while natural fire hazard has temperature rising rapidly gaining a peak temperature and then depending upon fuel available this temperature starts declining. For Structural fire Design to replicate the Natural Fire Curve one would utilize the Parametric Fire Curve also known as Design Fire Curve given in EN 1992 [9]. Parametric fire curve depends on various factors like the fuel load density, opening factors, fire duration, fire intensity, suppression systems, compartment size and geometry.

For the experiment purpose mostly Standard fire curves proposed by ISO 834 [10] and ASTM E119 [11] are used. ISO 834 curve is represented by equation (1). Unlike Natural fire, these temperature-time curves show rising temperature while a natural fire attains a peak temperature and then declines. Standard fire curves give a more conservative design whereas for an understanding of realistic behaviour Design parametric fire curve can be used as proposed by Eurocode and iBMB fire curve by Zefus & Hosser [12]. The figure below shows a comparison of the Standard Fire Curve and the Design Fire Curve.

$$T = 20 + 345 * \log_{10}(8t + 1) \qquad (1)$$
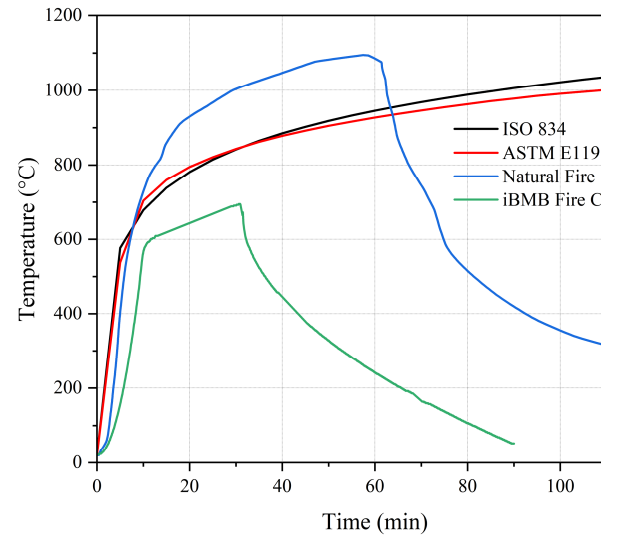$$\text{where, t is time in minutes [10]}$$

Fig. 2 ISO 834 vs ASTM E119 vs Natural Fire vs iBMB fire curve [10], [11], [12].

II. MATERIAL AND METHOD

The Most important parameters for Finite Element Analysis are the mechanical properties of materials at elevated temperatures. Different materials like concrete, reinforcing steel, and tendons behave differently in fire. The parameters that control the concrete behaviour like compressive and tensile strengths, modulus of elasticity, creep strain, thermal conductivity and thermal strain are non-linear functions of temperature [13].

A. Concrete Compressive Strength

The most important effects of elevated temperature on concrete are the dehydration of the cement paste, an increase in porosity, modifications in the moisture content, thermal expansion, alteration of pore pressure, loss of strength, thermal cracking due to incompatibility, thermal creep and thermal spalling due to excessive pore pressure. Water distribution and transport, whether in a gaseous or liquid form, play important roles in the local damage to concrete structures [14]. Strength and Serviceability criteria any concrete structure is affected in case of fire. The behaviour of a concrete structural member exposed to fire is dependent, in part, on the thermal, mechanical, and deformation properties of the concrete to which the member is composed. Similar to other materials the thermophysical, mechanical, and deformation properties of concrete change substantially within the temperature range associated with building fires [15]. The mechanical properties of concrete at elevated temperatures are of primary interest like compressive strength, tensile strength, stress-strain response and modulus of elasticity. Although compressive strength is of most concern as concrete is used for its high compressive strengths and loss may lead to localized or even global collapse of respective structures like columns. Many studies have been performed and various equations have been proposed to calculate the compressive strength of concrete as in the table below.

138

EN 1992-1-2-2004 [9]	$f'cT = f'c \ \ T \leq 100℃$ $f'cT = f'c \ (1.067 - 0.00067T) \ \ 100℃ \leq T \leq 400℃$ $f'cT = f'c(1.44 - 0.0016T) \ \ T \geq 400℃$
ASCE manual (1992) [16]	$f'cT = f'c \ \ 20℃ \leq T \leq 450℃$ $f'cT = f'c \left(2.011 - 2.353\left(\dfrac{T-20}{1000}\right)\right) \ \ 450℃ \leq T \leq 874℃$ $f'cT = 0 \ \ \ T \geq 874℃$
Rokade et al (2022) [17]	$f'cT = f'c \ (0.9841 - 0.0002T - (1 \times 10^{-6})T^2) \ \ 0℃ \leq T \leq 800℃$ $f'cT = 0 \ \ \ T \geq 800℃$
Chang et al. (2006) [18]	$f'cT = f'c \ (1.01 - 0.00055T) \ \ 20℃ \leq T \leq 200℃$ $f'cT = f'c \ (1.15 - 0.00125T) \ \ 200℃ \leq T \leq 800℃$
Kodur et al . (2004) [19]	$f'cT = f'c \ (1 - 0.003125(T - 20)) \ T \leq 100℃$ $f'cT = 0.75 \ f'c \ \ 100℃ \leq T \leq 400℃$ $f'cT = f'c(1.33 - 0.00145T) \ \ T \geq 400℃$
Lie et al. (1986) [20]	$f'cT = f'c \ (1 - 0.001T) \ T \leq 500℃$ $f'cT = f'c(1.375 - 0.00175T) \ \ 500℃ \leq T \leq 700℃$ $f'cT = 0 \ \ T \geq 700℃$

Fig. 3 Variation of Compressive Strength with temperature from various models

B. Concrete Tensile Strength

Although while designing RC structures at room temperature the tensile strength is neglected as it is only about 10% but in case of Fire Design tensile strength is one of the most important criteria.Concrete is weak in tension and for NSC, tensile strength is only 10% of its compressive strength and for HSC, tensile strength is further reduced [15]. However, from fire resistance point of view, it is an important property, because cracking in concrete is generally due to tensile stresses and the structural damage of the member in tension is often generated by progression in micro-cracking [21]. Under fire conditions, tensile strength of concrete can be even more crucial which may lead to spalling in concrete members [22]. Various models to predict the loss of tensile strength are given below.

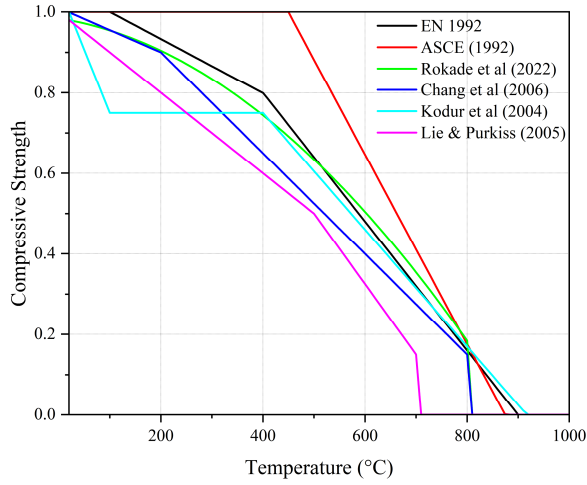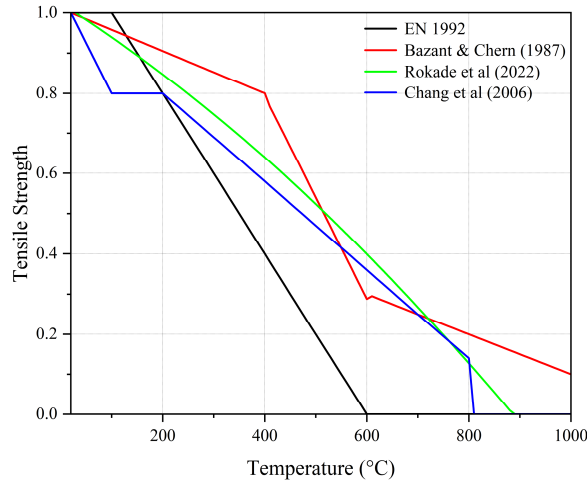| EN 1992-1-2-2004[9]	$f_{ck,t}T = k_{c,t} * f_{ck,t}$ $k_{c,t} = 1 \ 20℃ \leq T \leq 100℃$ $k_{c,t} = 1 - \left(\dfrac{T-100}{500}\right) \ \ 100℃ \leq T \leq 600℃$
Bazant and Chem (1987)[14]	$f_{ck,t}T = f_{ck,t}(1.01052 - 0.000526T) \ 20℃ \leq T \leq 400℃$ $f_{cr,t}T = f_{ck,t}(1.8 - 0.00252T) \ 400℃ \leq T \leq 600℃$ $f_{ck,t}T = f_{ck,t}(0.6 - 0.0005T) \ 600℃ \leq T \leq 1000℃$
Rokade et al (2022)[17]	$f_{ck,t}T = f_{ck,t}(1.0234 - 0.0008T - (4 \times 10^{-7}) T^2) \ 0℃ \leq T \leq 900℃$
Chang et al. (2006)[18]	$f_{ck,t}T = f_{ck,t}(1.05 - 0.0025T) \ 20℃ \leq T \leq 100℃$ $f_{ck,t}T = 0.80 f_{ck,t} \ 100℃ \leq T \leq 200℃$ $f_{ck,t}T = f_{ck,t}(1.02 - 0.0011T) \ 200℃ \leq T \leq 800℃$

Fig. 4 Variation of Tensile Strength with temperature from various models

TABLE III
MATHEMATICAL MODELS FOR TEMPERATURE DEPENDENT YOUNGS MODULUS OF CONCRETE

Bazant and Chem (1987) [14]	$E_{cT} = E_c\big(1 - (1.256 \times 10^{-3}T)\big)\ T \leq 650°C$ $E_{cT} = E_c\big(0.1837 - (0.5656 \times 10^{-3}(T - 650))\big)\ 650°C < T \leq 800°C$
Lie & Purkiss (2005) [25]	$E_{cT} = E_c\left(\dfrac{800 - T}{740}\right) \leq E_c\ \ 20°C \leq T \leq 1000°C$
Chang et al 2006 [18]	$E_{cT} = E_c\big(1.033 - (1.65 \times 10^{-3}T)\big)\ 20°C \leq T \leq 600°C$
Rokade et al (2022) [17]	$E_{cT} = E_c(1.0309 - 0.0015T - (4 \times 10^{-7}))\ 0°C \leq T \leq 900°C$
BS 8110-1(1997) [26]	$E_{cT} = E_c\left(\dfrac{700 - T}{550}\right) \leq E_c\ \ 20°C \leq T \leq 1000°C$

C. Concrete Elastic Modulus

Modulus of Elasticity of concrete is widely used to analyse RC structures to check the stresses, moments developed in structure and the deflections occurring to elements. At elevated temperatures, studies have shown a rapid reduction of the elastic modulus of concrete causing increased stress in elements. The modulus of elasticity decreases rapidly with the rise of temperature, and the fractional decline does not depend significantly on the type of aggregate [23]. Various models to show reduction in elastic modulus are given below. The modulus of elasticity (E) of various concretes at room temperature varies over a wide range, 5.0×103 to 35.0×103 MPa, and is dependent mainly on the water-cement ratio in the mixture, the age of concrete, the method of conditioning, and the amount and nature of the aggregates [24].
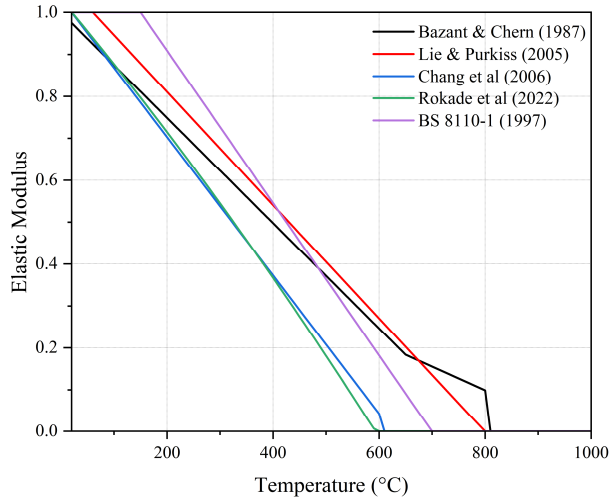

Fig. 5 Variation of Elastic Youngs Modulus with temperature from various models

D. Concrete Stress-Strain Curves for Compressive Strength

For the Numerical analysis of concrete, its behaviour under loading is expressed in the form of stress-strain curves. These stress-strain curves as used as input in Finite Element Software to simulate the actual behaviour of that material. At elevated temperatures, the degradation of compressive and increase in strain is given in EN 1992 2004 [9]. This model can be used to draw the stress-strain curve of the compressive strength of concrete. The model for compressive strength of Concrete as per EN 1992 [9] is given below.
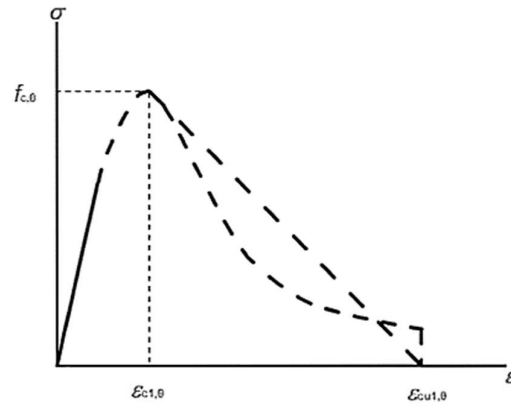

Fig. 6 Temperature Dependent Stress Strain Curve for Compressive Strength of Concrete as per EN 1992- 2004 [5]

140

TABLE IV
TEMPERATURE DEPENDENT STRESS STRAIN CURVE FOR COMPRESSIVE STRENGTH OF CONCRETE AS PER EN 1992

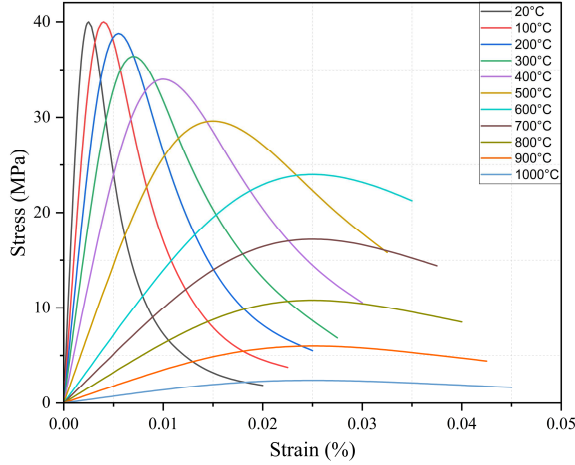|	
$$\sigma_c = \dfrac{3\varepsilon f'cT}{\varepsilon_{c1,\theta}\left(2 + \left(\dfrac{\varepsilon}{\varepsilon_{c1,\theta}}\right)^3\right)}$$	$\varepsilon \le \varepsilon_{cu1,\theta}$
Linear or Non-linear descending branches are permitted for numerical purposes for range	$\varepsilon_{c1,\theta} < \varepsilon \le \varepsilon_{cu1,\theta}$

Fig. 7 M40 Stress Strain curve as per EN 1992- 2004 [5]

E. Reinforcement Stress Strain Curves

Concrete is weak in tension so reinforcement is the form of rebars and tendons used to carry the tensile stresses in RC structures. To model the behaviour of reinforcement at elevated temperatures EuroCode [9] has given us stress-strain curves for reinforcement and tendons. The critical temperature at which the strength gets reduced by 50% for prestressing steel ranges from 300 to 500 ◦C[8][27][28][29]. The critical temperature for prestressing steel also depends upon the stress induced during its service life. Initial prestress is found to have a significant effect on yield and ultimate strength of tendons beyond 450 ◦C[28]. Eurocode equations represent stress-strain curves for both reinforcement and tendons as trilinear curves which may not be real representations and other models can be used to more accurately map the stress-strain curves.

TABLE V
MATHEMATICAL MODELS FOR TEMPERATURE DEPENDENT STRESS STRAIN CURVES OF REINFORCEMENT AND PRESTRESS TENDONS AS PER EN 1992-1-2 2004 [9]

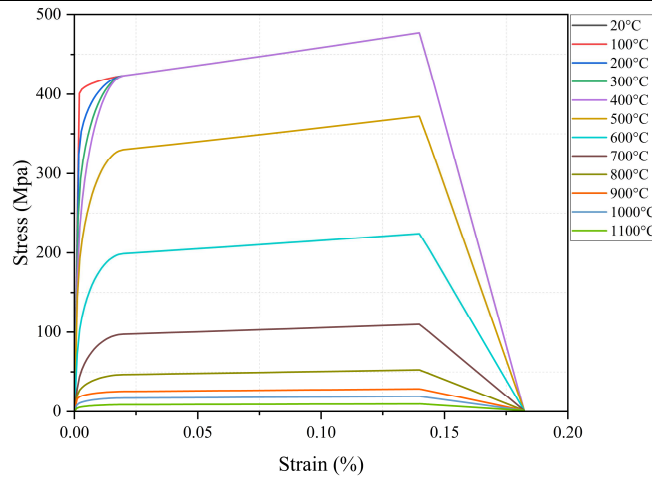|	
$\sigma_\theta = \varepsilon E_{s,\theta}$	$\varepsilon = \varepsilon_{sp,\theta}$
$\sigma_\theta = f_{sp,\theta} - c + \left(\dfrac{b}{a}\right)\left[a^2 - \left(\varepsilon_{sy,\theta} - \varepsilon\right)^2\right]^{0.5}$ Where, $a^2 = \left(\varepsilon_{sy,\theta} - \varepsilon_{sp,\theta}\right) * \left(\varepsilon_{sy,\theta} - \varepsilon_{sp,\theta} + \dfrac{c}{E_{s,\theta}}\right)$, $b^2 = c\left(\varepsilon_{sy,\theta} - \varepsilon_{sp,\theta}\right)E_{s,\theta} + c^2$, $c = \dfrac{\left(f_{sy,\theta} - f_{sp,\theta}\right)^2}{\left(\varepsilon_{sy,\theta} - \varepsilon_{sp,\theta}\right)E_{s,\theta} - 2\left(f_{sy,\theta} - f_{sp,\theta}\right)}$ & $\varepsilon_{sp,\theta} = \dfrac{f_{sp,\theta}}{E_{s,\theta}}$	$\varepsilon_{sp,\theta} \le \varepsilon \le \varepsilon_{sy,\theta}$
$\sigma_\theta = f_{sy,\theta}$	$\varepsilon_{sy,\theta} \le \varepsilon \le \varepsilon_{st,\theta}$
$\sigma_\theta = f_{sy,\theta}\left(\dfrac{1 - \left(\varepsilon - \varepsilon_{st,\theta}\right)}{\varepsilon_{su,\theta} - \varepsilon_{st,\theta}}\right)$	$\varepsilon_{st,\theta} \le \varepsilon \le \varepsilon_{su,\theta}$
$\sigma_\theta = 0$	$\varepsilon = \varepsilon_{su,\theta}$

Fig. 8 Stress Strain curve for Reinforcing bar as per EN 1992- 2004 [5]

141

The above model is also suitable for Prestress Tendons which is a tri linear model for tendons, a quad-linear model proposed by Shakya [28] is given below. This proposed model is valid for $20^0C \leq T \leq 800^0C$.

TABLE VI
MATHEMATICAL MODELS FOR TEMPERATURE DEPENDENT STRESS STRAIN CURVES OF PRESTRESS TENDONS [28]

$\sigma = E_T * \varepsilon$	$0 \leq \varepsilon \leq \dfrac{\sigma_{PT}}{E_T}$
$\sigma = \dfrac{\sigma_{yT} - \sigma_{pT}}{\varepsilon - \dfrac{\sigma_{PT}}{E_T}} * \left(\varepsilon - \dfrac{\sigma_{PT}}{E_T} \right)$	$\dfrac{\sigma_{PT}}{E_T} < \varepsilon < \varepsilon_{yT}$
$\sigma = \dfrac{\sigma_{uT} - \sigma_{yT}}{\varepsilon_{uT} - \varepsilon_{yT}} * \left(\varepsilon - \varepsilon_{yT} + \sigma_{0.2T} \right)$	$\varepsilon_{0.2T} < \varepsilon < \varepsilon_{uT}$
$\sigma = \dfrac{\sigma_{kT} - \sigma_{uT}}{\varepsilon_{kT} - \varepsilon_{uT}} * \left(\varepsilon - \varepsilon_{uT} + \sigma_{uT} \right)$	$\varepsilon_{uT} < \varepsilon < \varepsilon_{kT}$

Where,

$$\frac{\sigma_{yT}}{\sigma_y} = 6^{-12} * T^4 - 6^{-09} * T^3 - 9^{-08} * T^2 - 6^{-04} * T + 1.0196 \tag{2}$$

$$\frac{\sigma_{uT}}{\sigma_y} = 1^{-12} * T^4 - 3^{-09} * T^3 - 6^{-06} * T^2 + 6^{-04} * T + 0.9895 \tag{3}$$

$$\frac{\varepsilon_{kT}}{\varepsilon_k} = -7^{-11} * T^4 + 1^{-07} * T^3 - 6^{-05} * T^2 + 8.2^{-03} * T + 0.8276 \tag{4}$$

$$\frac{E_T}{E} = 7^{-12} * T^4 - 9^{-09} * T^3 + 2^{-06} * T^2 - 2^{-04} * T + 1.0099 \tag{5}$$
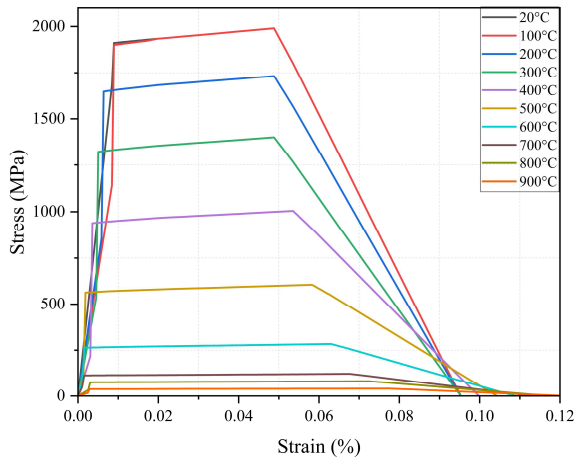

Fig. 9 Tendon Stress Strain curve as per EN 1992- 2004 [5]
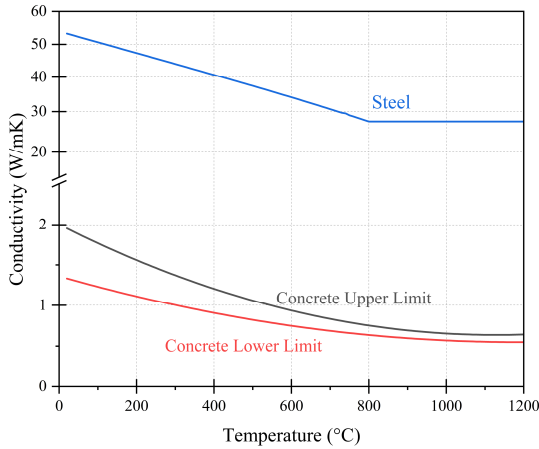
F. Thermal Properties

Fig. 10 Conductivity of Concrete and Steel [9], [30]

Temperature dependent Thermal Properties used for simulation are conductivity, specific heat and thermal elongation for concrete and reinforcement (bars and strands). The temperature dependent properties were derived from EN 1992-2004[9] for concrete and EN 1993-2005[30] for steel. For concrete specific heat values for 3% moisture content were used while lower limit of conductivity was used. Thermal Elongation of calcareous aggregate in slightly less than compared to silicaceous aggregate hence later one is used.
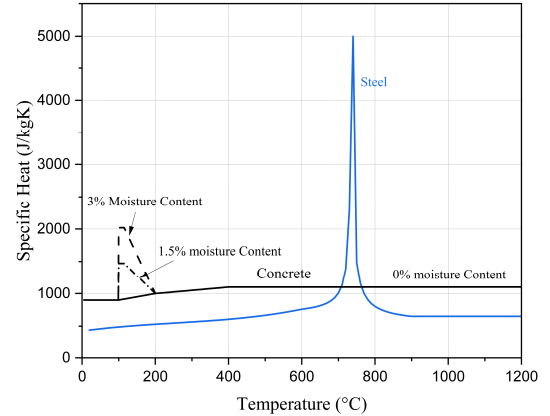

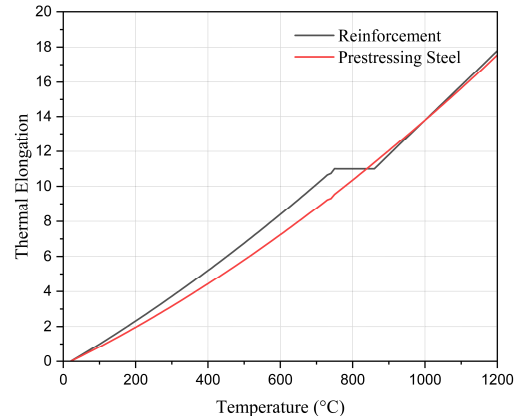Fig. 11 Specific Heat of Concrete and Steel [9] , [30]

Fig. 12 Thermal Elongation of Reinforcement and Prestressing Steel EN 1993- 2005[30]
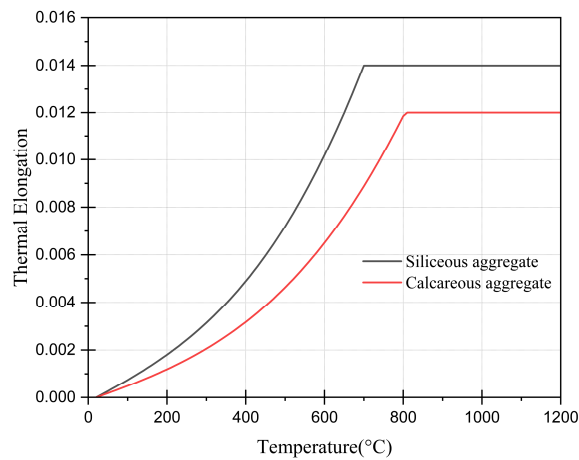
Fig. 13 Thermal Elongation of Concrete EN 1992- 2004 [9]

G. Case Study

Reinforced Concrete beam tested by Dwaikt and Kodur [31] was used to test FEM analysis. This test was chosen due to the comprehensive results reported by the two authors, which aids in conducting finite element simulations and making detailed comparisons.

1) Test by Dwaikt and kodur[31]

The beam tested was 3960 mm long with a cross-section of 254 mm x 406 mm. The beam was reinforced with three 19 mm diameter bars for tensile strength and two 13 mm diameter bars for compressive strength. The shear reinforcement consisted of 6 mm diameter stirrups spaced 150 mm apart along the length of the beam. The specified yield strengths for the main reinforcing bars and stirrups were 420 MPa and 280 MPa, respectively. The bottom and side clear cover provided was 38 mm and 50 mm at the top. The cylinder compressive strength of concrete was 52.2 MPa on the day of testing.

The beam was simply supported at a distance of 3660 mm from centre to centre. Two point loads of 50kN were applied at a distance of 610 mm from the centre of the beam on both sides. Of the 3960 mm 2440 mm length was subjected to ASTM E119 Standard Fire [11]. In the fire tests, the authors applied loading 30 min before the start of the fire and this loading was maintained till no further increase in deformation could be measured. This was selected as the initial condition for the deflection of the beam. The load was then maintained constant throughout fire exposure. Beam B1 failed during fire exposure after 180 minutes [32]

2) Test by Park & Kang [33]

To check the efficiency of FEM in analysing Post Tensioed structures a slab tested by Park & Kang [33] was chosen for this study. They also validated the slab numerically hence this slab was chosen as numerical simulation results were available for comparison. The slab was 6700mm x 1500 mm with a depth of 250mm. The reinforcement configuration consists of two 13-mm diameter bars for the lower longitudinal reinforcement, two 10-mm bars for the upper longitudinal reinforcement, and 10-mm stirrups spaced 275 mm apart for transverse reinforcement. Additionally, six extra 10-mm hairpin bars and stirrups were placed at the ends to counteract post-tensioning stresses. The reinforcing bars had a yield strength of 400 MPa. The slab had six 15.2mm dia seven wire strands two per duct. The strands had an Ultimate strength of 1895 MPa and yield strength of 1670 MPa with Young's modulus of 200000 MPa. The compressive strength of the concrete used for the slab was 40 MPa.

The tendons had a parabolic profile with minimum eccentricity at the slab centre. A clear cover of 35mm was provided at the slab centre. The slab was subjected to ISO 834 standard fire curve [10] for its full width of 1500mm and length of 6000mm. The fire test was carried out for 2-hour exposure. The slab was subjected to 4 equally spaced point loads of 30kN each initially for 10 mins before the fire test which was kept constant throughout the fire test. The slab showed a rapid increase in deflection during the fire exposure.

- Finite Element Modelling

Numerical simulation was performed in FEA software Abaqus. The simulation was performed in two steps.1) Heat transfer analysis.2) Coupled temperature displacement analysis.All the thermal and mechanical properties required for simulation were derived from EucoCode.Temperature-dependent thermal conductivity, specific heat, and thermal elongation were the thermal properties defined for concrete, reinforcement and prestressed strands derived from EuroCode.

For Concrete EN 1992-1-2 2004 [9] was used while for steel EN 1993-1-2 2005 [30] was used. The mechanical properties of concrete were temperature-dependent density, elasticity and plasticity. The plasticity model for reinforcement and strands was the Ductile Damage evolution and Concrete damage Plasticity model for concrete.To account true behaviour of both materials the engineering stress-strain curve given in Eurocode must be converted to a true stress-strain curve or else numerical simulations will not converge. Ture stress can be calculated using the following equations $\sigma_{true} = \sigma_{eng}(1 + \varepsilon_{eng})$ And true strain can be calculated using $\varepsilon_{true} = \ln(1 + \varepsilon_{eng})$.

TABLE VII
CONCRETE DAMAGE PLASTICITY VARIABLES

Dilation angle (degrees)	Eccentricity	σb0=σc0	Kc	Viscosity
50	.1	1.16	.67	.005

- Heat Transfer Analysis.

The element used in the heat transfer of concrete is an eight-node linear brick heat transfer (DC3D8), and the meshed element type for reinforced bars and PT strands was a two-node heat transfer link (DC1D2).Conduction is defined as the transfer of heat through the body of a structure, whereas convection and radiation are defined as the transfer of heat at the structure's surface with surrounding conditions[34].In experimental tests, Convection and radiation were heat transfer mechanisms, to simulate them we need to apply surface film conditions and surface radiation interactions. Surface film condition with specified film coefficient is applied to fire-exposed surface and air-exposed surface. The sink temperature is kept at 1 and the desired fire curve is applied in the form of sink amplitude to interactions applied to fire exposed surface. In the case of radiation surface emissivity of 0.8 is applied to fire exposed surface to simulate

radiation. The temperature gradient in heat conduction is described by Fourier's differential equation [35].

$$\frac{\partial}{\partial x}\left(k\frac{\partial T}{\partial x}\right) + \frac{\partial}{\partial y}\left(k\frac{\partial T}{\partial y}\right) + \frac{\partial}{\partial z}\left(k\frac{\partial T}{\partial z}\right) + Q \tag{6}$$
$$= \rho c \frac{\partial T}{\partial t}$$

where c = specific heat capacity; k = conductivity; Q = inherently generated heat; and ρ = density. In the heat transfer analysis, the parameters for concrete and steel were defined as previously mentioned, and Q was negligible (Q = 0). The temperature gradient in heat convection and radiation is described by the Robin boundary condition [35]

$$-k\frac{\partial T}{\partial n} = h(T - T_f) \tag{7}$$
$$+ \sigma \varepsilon_m \varepsilon_f \left[(T - T_z)^4\right.$$
$$\left. - (T_f - T_z)^4\right]$$

where h = convective heat transfer coefficient; n =outward normal direction of member surface; T_f = measured fire temperature in furnace; T_z = absolute zero temperature (−273.15°C); σ is the Stefan–Boltzmann constant [5.67 × 10−8 W/m^{2}K]; ε_f =heat emissivity of fire for air exposed surface εf=1 ; and εm = heat emissivity of exposed surface whose value εm=0.8. EuroCode has a defined value of h for fire-exposed surface as 25 W/m^{2}K^4 and for the air-exposed surface as 9 W/m^{2}K.

- Coupled Thermomechanical Analysis-

Coupled Thermomechanical analysis is performed in 2 stages. In the first stage all loads are applied including gravity load and external loads for a specific duration then in the second stage the fire is applied using heat transfer mechanisms given in equations (6), (7) for a specific fire curve. This analysis simulates the behaviour of simultaneous fire and external loads. The duration of the second stage depends upon the exposure time used in the fire curve. This analysis gives temperatures and stress fields simultaneously. The element type used for concrete was 8 noded thermally

coupled brick elements (C3D8T) and a two-noded 3D Truss element for reinforcement and tendons (T3D2T). A perfect bond between reinforcement (bars and strands) was used using Embedded region constraint. As bonded tendons were used Embedded region was applied to tendons as well to form a perfect bond.

III. RESULTS AND DISCUSSION

A. Heat Transfer Analysis

In the case of the beam ASTM E 119 [11] fire curve was applied for 3 hours duration and temperature was measured at the beam bottom at the bottom main reinforcement and beam centre. In the case of slab ISO 834[10] fire curve was applied for 2 hours duration and temperature was measured at slab bottom at the bottom main reinforcement tendon at the slab centre. The heat transfer results are shown in the figure 14.

The ASTM Fire curve used in beam test by Kodur had slightly more temperature than the Fire Curve Proposed in ASTM E119 [11]. The difference in measured temperature in experiment and FEA analysis after 180 minutes of fire exposure was 17°C with error of 1.64 %.
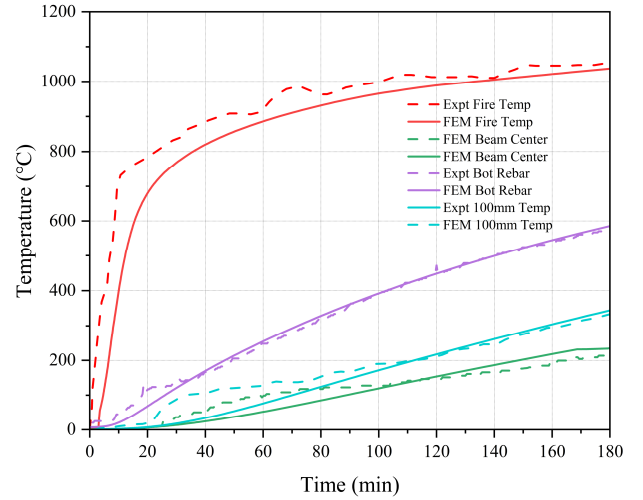

Fig. 14 Thermal Analysis Results of Beam by Kodur [31]

TABLE VIII
HEAT TRANSFER ANALYSIS RESULTS

Case Study	Location	Measured Temperature °C		% Error
		Experiment	FEM analysis	
Beam by Kodur[31]	Beam Bottom	1054	1037	1.64
	Bottom Reinforcement	593	585	1.35
	Beam 100mm	333	343	3
	Beam centre	214	235	9.8
PT Slab by Kang [33]	Slab Bottom	1024	1014	1
	Bottom Reinforcement	361	354	2
	Tendon at Centre	339	348	2.65

B. Coupled thermomechanical Analysis Results

The RC beam by Kodur [31] was loaded by 2-point loads for 3 hours for ASTM E119 [11] Fire Curve. While the PT slab was loaded by four point loads for 2 hours with ISO 834 standard Fire curve[10]. The Coupled Thermomechanical Analysis is plotted below. Fig 15 represents a comparison of Experimental Fire tests and FEM analysis of RC Beam by

Kodur [31] and Fig. 16 shows the comparison of the Experimental Fire Test and FEM analysis results of the PT slab by Kang [33].
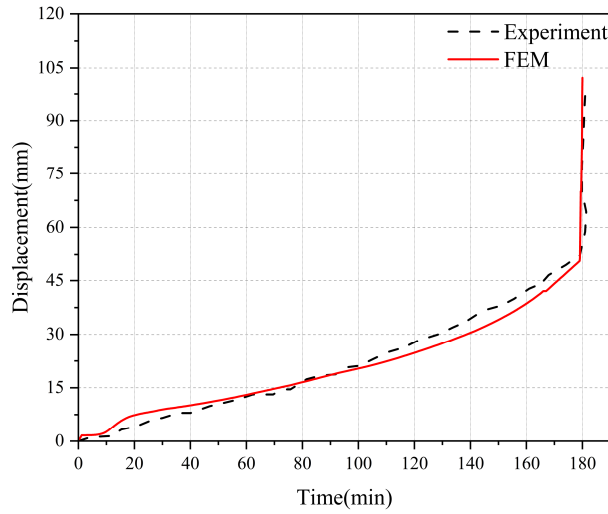
Fig. 15 Experimental and FEM comparison of Displacements of RC beam by Kodur [31]
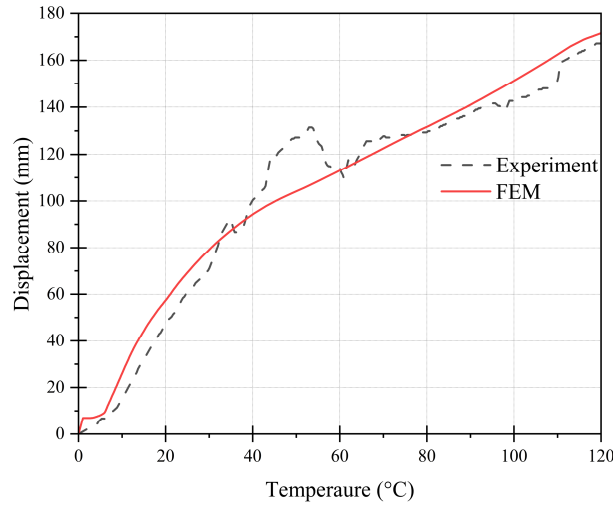

Fig. 16 Experiemental and FEM comparison of Displacements of PT Slab by Kang [33]
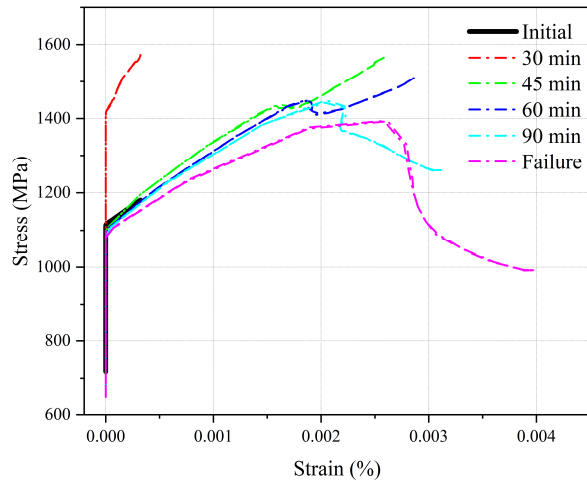

Fig. 17 Parametric Study of Tendon Stress-Strain Curve in PT Slab by Kang [33]

A parametric study of the Stress-Strain Curve for Tendons was also Performed using FEA software. The variation of stress with fire exposure time is represented in Fig 17. Initially, no strain was induced in tendons as the temperature rises the capacity of tendons decreases as per the material model proposed in Eurocode. While the load is constant during the analysis the stress in tendons reduces with temperature rise. After 60 minutes of fire exposure, the tendons reached ultimate strength and the ductile damage is seen. The ultimate strength of tendons was 1895 MPa but failure occurred at the ultimate strength of 1392 Mpa during the 2-hour fire exposure.

In the Experimental study of RC beam by Kodur[31] their was a sudden failure seen at 180 minutes of fire exposure. The damage to reinforcement was significant as the bottom reinforcement temperature reached 593°C which caused a reduction in the strength of the reinforcement. In the case of PT slab, the bottom reinforcement reached a maximum temperature of 361°C hence there was no complete loss of strength and no sudden failure was visible after 120 mins of fire exposure. In an experimental study of PT slab by Kang [33]sudden rise in displacement is seen between 40 to 60 minutes of fire exposure. This trend is not visible in Finite Element Analysis moreover the displacement gradually rises with exposed time.

TABLE IX
COUPLED THERMOMECHANICAL ANALYSIS RESULTS

Case Study	Measured Displacement (mm)		% Error
	Experiment	FEM analysis	
RC beam by Kodur [31]	97	103	6.1
PT Slab by kang [33]	167	173	3.7

IV. CONCLUSION

This study has investigated the adequacy of Finite Element Analysis in simulating the behaviour of RC beam and Poste Tensioned slab subjected to elevated temperature. This study confirms that Finite Element Analysis is highly capable of predicting the experimental tests in terms of heat transfer , deflection and predicting failure modes. The error found in the heat transfer analysis and coupled temperature displacement analysis is less than 10%.

The study identified that using proper models of materials at elevated temperature is very necessary in capturing the real world behaviour of structure. For capturing the behaviour of complex structures more advanced material models are required which capture the realistic behaviour. FEA is highly capable of doing a parametric study of materials to see their behaviour during fire exposure. This is necessary for predicting realistic behaviour at required time intervals.

Variations in the mesh sizes and type of mesh element used also have a major impact in predicting the behaviour. Decreasing mesh size increases the accuracy of results but comes with additional computational costs. The use of suitable boundary conditions, loads and interactions is required for good correlation of results.

This study only dealt with elements subjected to standard fire curves which do not contain the cooling part of fire curve. For understanding the material behaviour during cooling

phase,use of Design fire curves is suggested which will predict the peak temperatures and the duration upto which the fire lasts.

FEA analysis is not able to capture any defects present in materials which causes sudden variation in experimental results as seen in case Study of Post-tensioned Slab by Kang[33] where, between 40 to 60 minutes of fire exposure sudden rise and deflection was visible.

The use of Finite Element Analysis will be helpful in Fire Engineering as the need for physical fire tests is eliminated which saves resources as well as time. Moreover, the complex structures can be modelled using the various material models developed by researchers to help understand their failure mechanisms. Further study required is to model complete structures and more realistic material models for reinforcements to capture the failure behaviour of whole structures.

NOMENCLATURE

$f'cT$ Compressive Strength at Elevated Temperature.
$f'c$ Compressive strength at Normal Temperature.
$f_{ck,t}T$ Tensile Strength of Concrete at Elevated Temperature.
$f_{ck,t}$ Tensile Strength of Concrete at Normal Temperature.
E_{cT} Temperature Dependent Youngs Modulus of Concrete.
E_c Youngs Modulus of Concrete at Normal Temperature.

REFERENCES

[1]   U.S. Fire Administration, *Residential Building Fire Causes*, U.S. Fire Administration, Emmitsburg, MD, USA, 2022. [Online]. Available: https://www.usfa.fema.gov/statistics/residential-fires/causes.html.

[2]   V. Kodur, P. Kumar, and M. M. Rafi, "Fire hazard in buildings: Review, assessment and strategies for improving fire safety," *PSU Res. Rev.*, vol. 4, no. 1, pp. 1–23, 2019, doi: 10.1108/PRR-12-2018-0033.

[3]   A. Cowlard, A. Bittern, C. Abecassis-Empis, and J. Torero, "Fire safety design for tall buildings," *Procedia Eng.*, vol. 62, pp. 169–181, 2013, doi: 10.1016/j.proeng.2013.08.053.

[4]   T. M. Jeyashree, P. R. Kannan Rajkumar, and K. S. Satyanarayanan, "Developments and research on fire response behaviour of prestressed concrete members - A review," *J. Build. Eng.*, vol. 57, p. 104797, 2022, doi: 10.1016/j.jobe.2022.104797.

[5]   M. M. Drury, A. N. Kordosky, and S. E. Quiel, "Robustness of a partially restrained, partially composite steel floor beam to natural fire exposure: Novel validation and parametric analysis," *J. Build. Eng.*, vol. 44, p. 102533, 2021, doi: 10.1016/j.jobe.2021.102533.

[6]   H. Liu, Z. Y. Gao, Q. W. Liu, and J. L. Zhang, "Assessment and strengthening of a fire damaged prestressed concrete continuous girder bridge," *Mater. Struct.*, vol. 48, no. 1, pp. 81–87, Jan. 2015, doi: 10.1617/s11527-013-0168-4.

[7]   W. Zheng, X. Hou, and M. Xu, "Experiment and analysis on fire resistance of two-span unbonded prestressed concrete continuous slabs," *J. Build. Struct.*, vol. 28, no. 5, pp. 1–13, 2007.

[8]   X. Hou, W. Zheng, V. Kodur, and H. Sun, "Effect of temperature on mechanical properties of prestressing bars," *Constr. Build. Mater.*, vol. 61, pp. 24–32, 2014, doi: 10.1016/j.conbuildmat.2014.03.001.

[9]   European Committee for Standardization, *EN 1992-1-2:2004: Eurocode 2: Design of Concrete Structures - Part 1-2: General Rules - Structural Fire Design*, CEN, Brussels, Belgium, 2004.

[10]   International Organization for Standardization, *ISO 834-1:1999: Fire-resistance tests - Elements of building construction - Part 1: General requirements*, ISO, Geneva, Switzerland, 1999.

[11]   ASTM International, *ASTM E119-20: Standard Test Methods for Fire Tests of Building Construction and Materials*, ASTM, West Conshohocken, PA, USA, 2020.

[12]   J. Zehfuss and D. Hosser, "A parametric natural fire model for the structural fire design of multi-storey buildings," Fire Saf. J., vol. 42, no. 2, pp. 115–126, 2007, doi: 10.1016/j.firesaf.2006.08.004.

[13]   U. Diederichs, C. Ehm, A. Weber, and G. Becker, "Deformation behaviour of HTR-concrete under biaxial stresses and elevated temperatures," in *Proc. 9th Int. Conf. Struct. Mech. Reactor Technol. (SMiRT 9)*, Lausanne, Switzerland, 1987, pp. H13–H19.

[14]   Z. P. Bažant and J. C. Chern, "Stress-induced thermal and shrinkage strains in concrete," *J. Eng. Mech.*, vol. 113, no. 10, pp. 1493–1511, Oct. 1987, doi: 10.1061/(ASCE)0733-9399(1987)113:10(1493).

[15]   V. Kodur, "Properties of concrete at elevated temperatures," *ISRN Civ. Eng.*, vol. 2014, p. 468510, 2014, doi: 10.1155/2014/468510.

[16]   ASCE Committee on Fire Protection, *Structural Fire Protection*, ASCE, New York, NY, USA, 1992, doi: 10.1061/9780872628885.

[17]   M. Rokade, M. Gaikwad, S. Singh, and S. Kadam, "A simplified regression-based approach for concrete mechanical properties at elevated temperature," *Asian J. Civ. Eng.*, vol. 23, no. 7, pp. 1065–1085, 2022, doi: 10.1007/s42107-022-00469-1.

[18]   Y. F. Chang, Y. H. Chen, M. S. Sheu, and G. C. Yao, "Residual stress–strain relationship for concrete after exposure to high temperatures," *Cement Concrete Res.*, vol. 36, no. 10, pp. 1999–2005, Oct. 2006, doi: 10.1016/j.cemconres.2006.05.029.

[19]   V. K. R. Kodur, T. C. Wang, and F. P. Cheng, "Predicting the fire resistance behaviour of high strength concrete columns," Cement Concrete Compos., vol. 26, no. 2, pp. 141–153, Feb. 2004, doi:10.1016/S0958-9465(03)00089-1.

[20]   T. T. Lie, T. J. Rowe, and T. D. Lin, "Residual strength of fire-exposed reinforced concrete columns," *ACI Spec. Publ.*, vol. SP-92, pp. 153–174, 1986.

[21]   S. Mindess, Ed., Developments in the Formulation and Reinforcement of Concrete, 2nd ed. Sawston, U.K.: Woodhead Publishing, 2019.

[22]   W. Khaliq and V. Kodur, "High temperature mechanical properties of high-strength fly ash concrete with and without fibers," *ACI Mater. J.*, vol. 109, no. 6, pp. 663–672, Nov. 2012, doi: 10.14359/51684164.

[23]   C. R. Cruz, "Elastic properties of concrete at high temperatures," *J. PCA Res. Develop. Labs.*, vol. 8, no. 2, pp. 37–45, May 1966.

[24]   D. A. Krishna, R. S. Priyadarsini, and S. Narayanan, "Effect of elevated temperatures on the mechanical properties of concrete," *Procedia Struct. Integr.*, vol. 14, pp. 384–394, 2019, doi:10.1016/j.prostr.2019.05.047.

[25]   L. Y. Li and J. Purkiss, "Stress–strain constitutive equations of concrete material at elevated temperatures," *Fire Saf. J.*, vol. 40, no. 7, pp. 669–686, 2005, doi: 10.1016/j.firesaf.2005.06.003.

[26]   British Standards Institution, *BS 8110-1:1997: Structural use of concrete - Part 1: Code of practice for design and construction*, BSI, London, U.K., 1997.

[27]   J. M. Atienza and M. Elices, "Behavior of prestressing steels after a simulated fire: Fire-induced damages," *Constr. Build. Mater.*, vol. 23, no. 8, pp. 2932–2940, Aug. 2009, doi:10.1016/j.conbuildmat.2009.02.024.

[28]   A. M. Shakya and V. K. R. Kodur, "Effect of temperature on the mechanical properties of low relaxation seven-wire prestressing strand," *Constr. Build. Mater.*, vol. 124, pp. 74–84, 2016, doi:10.1016/j.conbuildmat.2016.07.080.

[29]   Z. Tao, "Mechanical properties of prestressing steel after fire exposure," *Mater. Struct.*, vol. 48, no. 9, pp. 3037–3047, Sep. 2015, doi: 10.1617/s11527-014-0377-5.

[30]   European Committee for Standardization, *EN 1993-1-2:2005: Eurocode 3: Design of steel structures - Part 1-2: General rules - Structural fire design*, CEN, Brussels, Belgium, 2005.

[31]   M. B. Dwaikat and V. K. R. Kodur, "Response of restrained concrete beams under design fire exposure," *J. Struct. Eng.*, vol. 137, no. 9, pp. 953–963, Sep. 2011, doi: 10.1061/(ASCE)ST.1943-541X.0000358.

[32]   V. K. R. Kodur and A. Agrawal, "An approach for evaluating residual capacity of reinforced concrete beams exposed to fire," *Eng. Struct.*, vol. 110, pp. 293–306, 2016, doi:10.1016/j.engstruct.2015.11.047.

[33]   S. Park and T. H. K. Kang, "Experimental and numerical study of fire endurance of bonded posttensioned concrete slabs," *J. Struct. Eng.*, vol. 149, no. 12, p. 04023177, Dec. 2023, doi:10.1061/JSENDH.STENG-12384.

[34]   W. Y. Gao, J. G. Dai, J. G. Teng, and G. M. Chen, "Finite element modeling of reinforced concrete beams exposed to fire," *Eng. Struct.*, vol. 52, pp. 488–501, Jul. 2013, doi: 10.1016/j.engstruct.2013.03.017.

[35]   J. A. Purkiss and L.-Y. Li, *Fire Safety Engineering Design of Structures*, 3rd ed. Boca Raton, FL, USA: CRC Press, 2013, doi:10.1201/b16059.